AJNR

Isolated cysticercal infestation of extraocular muscles: CT and MR findings.

M A Ursekar, D K Dastur, D K Manghani and A T Ursekar

AJNR Am J Neuroradiol 1998, 19 (1) 109-113
http://www.ajnr.org/content/19/1/109

AJNR Am J Neuroradiol 19:109–113, January 1998

Isolated Cysticercal Infestation of Extraocular Muscles: CT and MR Findings

Meher A. Ursekar, Darab K. Dastur, Daya K. Manghani, and Atul T. Ursekar

PURPOSE: **We sought to document the appearance of isolated cysticercal infestation of single extraocular muscles on MR and CT studies, and to compare these findings with results of histopathologic examination.**

METHODS: **Six MR and three CT examinations of the orbits of six patients were reviewed. Histopathologic confirmation of the diagnosis was available in three patients, and response to specific medical therapy was available in one. In all, the imaging findings were considered highly suggestive of cysticercal infestation.**

RESULTS: **Typically, the affected extraocular muscle showed fusiform enlargement of its belly and contained a well-defined, spherical cyst with a nodule attached to its wall. The mural nodule was identified in all six cases with varying degrees of visibility. It was best seen on the CT examinations and in all cases in which contrast material had been administered. The nodule and the enlarged muscle showed intense enhancement on the contrast-enhanced studies. Imaging studies of the brain showed no evidence of cerebral cysticerci in any of the patients.**

CONCLUSION: **The MR and CT appearance of isolated infestation of single extraocular muscles by the larva of the pork tapeworm *Taenia solium* is quite characteristic and often diagnostic of this condition.**

Disseminated cysticercosis results from infestation with the larval stage of the pork tapeworm, *Taenia solium.* Common sites of involvement include the central nervous system (CNS), skeletal muscles, and subcutaneous tissue (1). Extraocular, orbital cysticercosis is uncommon, despite the frequency of ocular and brain involvement (2). Intraocular infection is often associated with generalized systemic infestation (2). We report six cases of cysticercosis of single extraocular muscles in which there was no evidence of CNS or subcutaneous involvement.

Methods

Six patients were chosen for this study from among those who underwent magnetic resonance (MR) imaging or computed tomography (CT) of the orbit and/or brain at our institution during a 2-year period. The six patients included all those in whom orbital cysticercosis was found. It would be appropriate to mention that this is a relatively small number compared with the large number of patients (approximately 400) who were imaged and found to have intracranial cysticercosis without orbital involvement. Three subjects were male and three female, ranging in age from 16 to 33 years. All six had MR examinations and three also had CT examinations of the orbit. Imaging of the brain was performed in every patient. All were referred with clinical signs of moderate to severe orbital inflammation and all had reported headache and orbital pain. Diplopia resulting from restricted extraocular movements occurred in all. Two patients, both with inferior rectus involvement, had proptosis. The duration of symptoms was 2 months to 1 year. Results of anterior segment and ocular fundus examination were normal in every patient. No patient had clinical signs of CNS involvement or palpable subcutaneous nodules.

All MR studies were performed on a 1.5-T system with the standard quadrature head coil. The affected orbit was examined with unenhanced T1-weighted spin-echo sequences in the axial, coronal, and sagittal oblique planes in five patients; one patient had imaging only in the coronal plane. Section thickness varied from 3 to 4 mm, and the field of view varied from 16 to 18 cm; matrix size was 256 × 192. Gadopentetate dimeglumine (0.1 mmol/kg) was injected in four patients. Contrast-enhanced studies were obtained in multiple planes, using fat-suppressed T1-weighted spin-echo sequences. All patients had T2-weighted imaging of the orbits in the axial or coronal plane, and standard cranial MR studies.

Unenhanced and enhanced CT examinations of the orbits were performed in the axial and coronal planes in three patients, using a Siemens (Erlangen, Germany) Hi-Q scanner. All scans were obtained with a section thickness of 2 to 3 mm in 2- to 3-mm increments.

In three of the six patients, the cyst was surgically excised, and histopathologic confirmation of the diagnosis was available. Postoperative CT examinations in these patients showed no evidence of any cystic remnant within the affected muscle.

Received November 15, 1996; accepted after revision May 30, 1997.

From the Departments of Neuroradiology (M.A.U.) and Neuropathology and Applied Biology (D.K.D., D.K.M.), Bombay Hospital & Institute of Medical Sciences, and the Department of Ophthalmology, Jaslok Hospital & Medical Research Center (A.T.U.), Bombay, India.

Address reprint requests to Meher A. Ursekar, Consultant Radiologist, Departments of Neuroradiology and MRI, Bombay Hospital, 12 Marine Lines, Bombay 400 020, India.

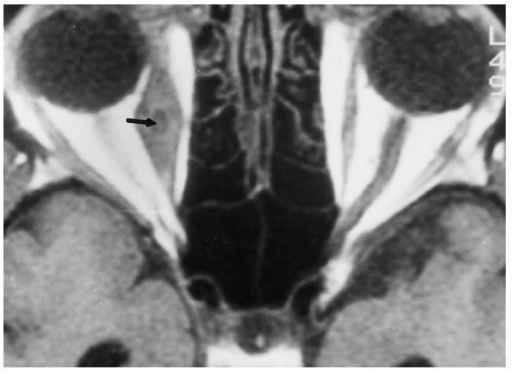

FIG 1. Axial T1-weighted (430/17/2 [repetition time/echo time/excitations]) MR image of the orbits shows fusiform expansion of the right medial rectus. The expanded muscle contains a sharply circumscribed cyst with a small mural nodule (*arrow*). The cyst wall appears slightly hyperintense relative to surrounding muscle.

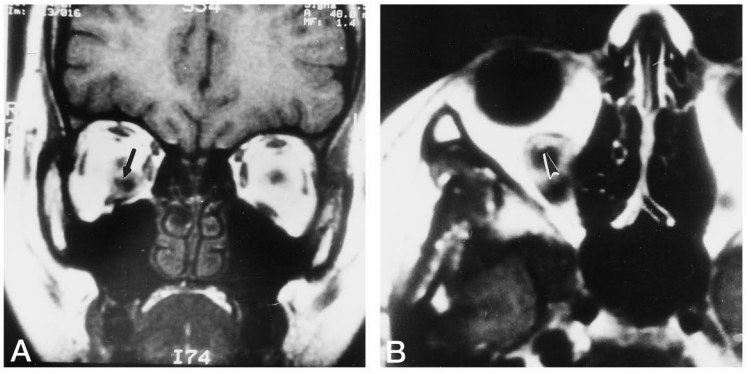

FIG 2. *A*, Unenhanced coronal T1-weighted (420/19/2) MR image of the orbits shows a cyst in the right inferior rectus. The mural nodule is poorly seen in this case as a focal protrusion into the cyst at its superior wall (*arrow*). The nodule was more clearly depicted on contrast-enhanced T1-weighted images obtained in the axial plane (see *B*).

B, Contrast-enhanced axial T1-weighted (420/19/2) image of the same patient enlarged to show the right orbit only. The enhancing nodule (*arrowhead*) is more conspicuous after contrast administration and is seen better in the axial plane.

Of the remaining patients, in one, the imaging findings were thought to be characteristic, and the patient was administered cysticidal drugs, after which the signs and symptoms of orbital inflammation regressed. The patient refused further imaging, and a presumptive diagnosis of cysticercal infection was made on the basis of typical imaging findings and clinical response to specific therapy. A presumptive diagnosis was made in the other two patients on the basis of the imaging appearance, which was thought to be typical.

Results

MR and CT Studies

MR images showed fusiform enlargement of the belly of the affected extraocular muscle, produced by a spherical or oval cyst, which was always well demarcated from surrounding muscle tissue. The cysts varied in size, with the smallest measuring 5 mm and the largest 10 mm in maximum diameter. The cyst was usually situated at the center of the muscle belly, except in one patient in whom it was eccentrically placed and jutted out into the orbital fat. The anterior tendinous insertions appeared normal in three, but were thickened in the remaining three. On T1-weighted images, the cystic fluid appeared isointense with normal vitreous and hypointense relative to surrounding muscle. A well-delineated peripheral hyperintense rim was seen in some cases. A nodule that was isointense with muscle was seen attached to the cyst wall in every case, with greater or lesser degrees of visibility (Fig 1). The nodule, although present, was not clearly depicted in two patients (Fig 2A). In both these patients the unenhanced MR studies were limited in spatial resolution because of the thicker sections and larger fields of view used. In one patient, the study was considered incomplete, as only coronal images were available. The conspicuity of the nodule increased in both patients after contrast administration, and, in one of them, when images were obtained in another plane (Fig 2B). On T2-weighted images, the cystic fluid was as hyperintense as the vitreous, while the mural nodule and peripheral rim appeared relatively hypointense (Fig 3). The mural nodule and the muscle belly showed intense enhancement after contrast administration (Fig 4).

The unenhanced and contrast-enhanced CT studies showed similar findings. The density of the cystic fluid was the same as the vitreous, while the mural nodule appeared relatively hyperdense and could be identified clearly in all three patients who underwent CT studies. In two contrast-enhanced studies, more than one internal structure could be identified, consisting of a nodule and a curved linear structure attached to the cyst wall (Fig 5).

Histopathology

Macroscopically, the cyst had a circular white spot, the "milk spot," surrounded by translucent fluid material (Fig 6, left). The fluid was straw-colored and had a protein content of 4.5 g/dL. Histopathologic examination of the milk spot revealed an invaginated larval parasite with a rostellum, suckers, hooklets, and the body of the larva (Fig 7A). The translucent material showed mainly the spiral canal. Although the whole cyst was found to be within the muscle at surgery, only small pieces of fibrous tissue were available for histopathologic examination (Fig 6, right). Microscopic examination of these pieces showed mononuclear cells, suggesting chronic inflammatory reaction, within a homogeneous fibrous matrix (Fig 7B).

Discussion

Teniasis is a parasitic disease with a worldwide distribution, which is endemic in developing countries (3). *Cysticercus cellulosae* is the encysted larva of the pork tapeworm, *Taenia solium.* Ingestion of food con-

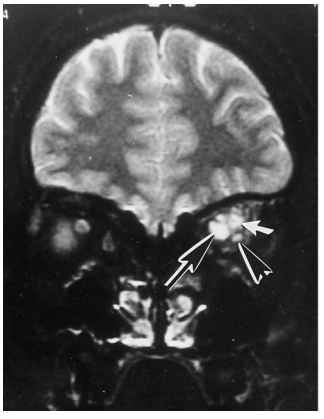

FIG 3. Coronal T2-weighted (2100/90/1) MR image of the orbits. The left superior rectus contains a spherical cyst with hyperintense fluid contents. The nodule (*small arrow*) and peripheral rim are relatively hypointense. The optic nerve (*arrowhead*) is displaced inferiorly, while the posterior aspect of the vitreous body (*large arrow*), which has entered the plane of section, lies medial to the cyst.

FIG 4. Contrast-enhanced T1-weighted (450/19/20) MR image shows intense enhancement of the mural nodule (*arrow*) and the cyst wall (*W*) with the adjacent inferior rectus muscle.

FIG 5. Contrast-enhanced coronal CT scan through a cyst in the right inferior rectus (of the same patient shown in Fig 2). A complex internal structure can be identified within the cyst, consisting of two nodules (*arrow* points to one nodule) and a curved linear structure (*arrowhead*).

taminated with the fertilized ova of *T solium* will induce cysticercosis in humans (4). The fertilized ova hatch in the small intestine, and the larvae penetrate the intestinal mucosa and migrate via the lymphatics or bloodstream to various organs. They may infest subcutaneous tissue, the CNS, the eye, muscle, liver, lung, heart, or peritoneum (5), but have a particular affinity for the muscles and the nervous system (4). Intraocular infection occurs when the larva enters the choroidal circulation (6). Larval death in ocular structures can produce severe inflammation, which may result in blindness (2). While intraocular infections are not uncommon, extraocular orbital involvement is rare (2). We encountered only six cases over a period of 2 years, as opposed to 400 others with isolated intracranial disease. The larvae may lodge in the eyelid (7–11), subconjunctival space (8), orbital tissue, or lacrimal gland (10). Reports of extraocular muscle involvement are exceptional (12–14).

Patients with extraocular cysticercosis usually present with clinical features suggesting subacute orbital myositis. In some patients, the presenting features mimic an orbital tumor (2). None of our patients had clinical or radiologic evidence of disseminated infection. The diagnosis in all cases was suggested by characteristic imaging findings.

Imaging of neurocysticercosis is well documented (1, 15–22). The appearance of brain parenchymal cysts depends on the stage at which they are detected during the course of their natural evolution (21). In a series of 32 patients with neurocysticercosis in whom CT and MR findings were correlated with pathomorphology, Lotz et al (22) described an early noncystic viable metacestode larval stage preceding the radiologically identifiable cystic stage. The noncystic larva

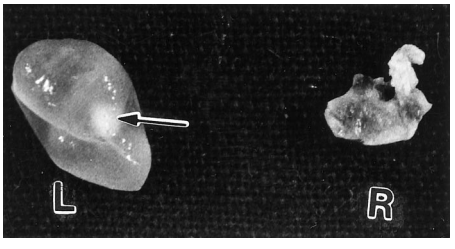

FIG 6. Histopathologic specimens show translucent cyst with a milk spot (*arrow*) (*left*) and fibrous tissue surrounding the cyst (*right*).

is invisible on CT and MR studies (22). The cystic stage (which represents the formation of an intact bladder worm or cystic metacestode larva) is easily recognized at imaging. The bladder is a distended cystic structure, 8 to 20 mm in size, that contains the invaginated protoscolex, an elongated opaque structure measuring 3×6 mm, free at one end and fixed to the wall at the other (22). Such "live cysts" have typical appearances and are identified as sharply circumscribed, nonenhancing, spherical cysts containing an internal structure or mural nodule (corresponding to the invaginated protoscolex) on imaging studies. The mural nodule may be round or elongated and curved, and is attached at one end to the cyst wall. The cystic fluid is clear so long as the larva is alive, and resembles cerebrospinal fluid or vitreous in density and MR signal intensity. Parasitic death results in pathoanatomic changes in the cyst and incites a host immune response consisting of pericystic inflammatory reaction. The degenerating protoscolex undergoes vacuolation and hyalinization (22), with a corresponding change in the imaging appearance. There is

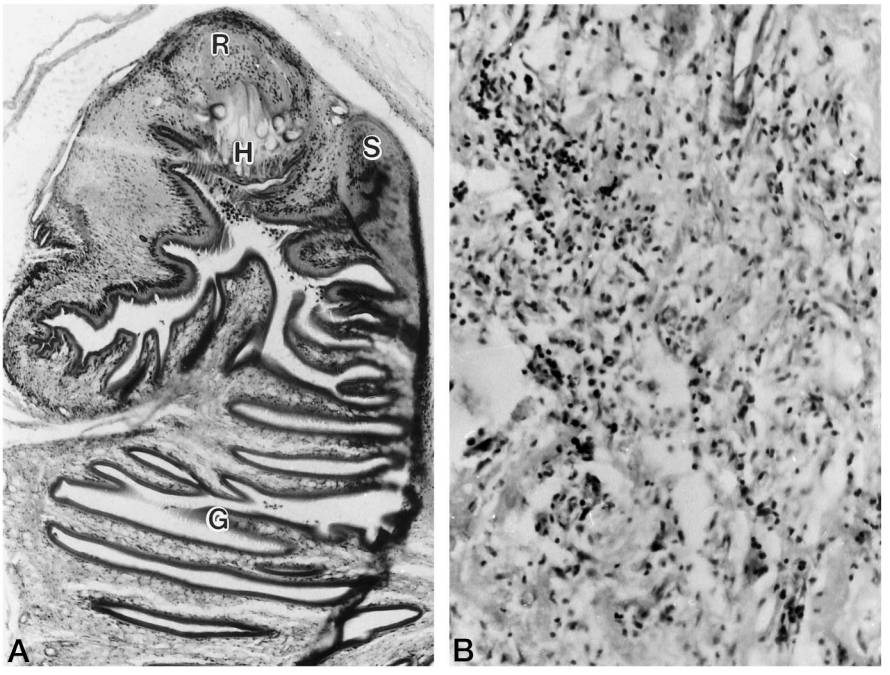

FIG 7. *A*, Photomicrograph of the milk spot seen in Figure 6 of the invaginated larval parasite shows a rostellum (*R*) with hooklets (*H*), sucker (*S*), and the body of the parasite occupied mainly by the gut (*G*) (hematoxylin-eosin, ×80).

B, Photomicrograph of the fibrous tissue seen in Figure 6 shows small and large mononuclear cells within a fibrous matrix (hematoxylin-eosin, ×160).

a variable degree of edema around the cyst and intense enhancement of its wall. We observed enhancement of the expanded muscle and its tendinous insertion (whenever it was involved) in all our cases, and, in one case, focal thickening and enhancement of the sclera at the site of tendinous insertion. Jena et al (1) observed changes in the signal-intensity characteristics of the mural nodule and cystic fluid on T1- and T2-weighted MR images in degenerating brain cysts. Viable cysts showed a hyperintense nodule and hypointense cystic fluid on T1-weighted images. The hypointense nodule was seen to contrast well with the hyperintense fluid on T2-weighted images. Degenerating cysts, on the other hand, showed progressive T2 shortening of the cystic fluid (1), probably due to increased turbidity and gelling of the fluid after larval death (15). The nodule showed progressive T1 and T2 lengthening, which was attributed to the greater free water content of the necrotic protoscolex (1). A hypointense rim or capsule may be visible on T2-weighted images of encapsulated, degenerating cysts (22). Over a variable period, dependent on the host immune response, the disintegrating larva evolves into a granulomatous abscess and eventually a mineralized nodule. Chronic abscesses contain pus and no identifiable protoscolex (22). On CT scans, they are isodense, ring-enhancing, or nodular enhancing lesions with or without edema (21, 23). On MR images, they appear as isointense to hypointense nodules on T1- and T2-weighted studies, and show progressive mineralization (24). During this stage, the lesions are radiologically indistinguishable from other infectious granulomas.

Cysticercal infestation of extraocular muscle can be presumptively diagnosed by the characteristic CT or MR appearance, especially before the stage of granulomatous abscess formation. The finding of a cyst containing a mural nodule is diagnostic. Because seeing the nodule is critical, every attempt should be made to increase its conspicuity on imaging studies. Pathologic descriptions emphasize its small size, which is usually 2 to 3 mm and sometimes up to 5 mm in diameter (15). Optimum visibility is, therefore, partly dependent on spatial resolution. In our experience, although limited to six cases, multiplanar imaging is usually necessary to see the nodule adequately. Use of intravenous contrast material was found to increase nodule conspicuity, as the nodule shows intense enhancement. Turbidity and gelling of the fluid after parasitic death and the resultant MR signal changes may reduce contrast between the nodule and the cystic fluid.

The diagnosis is elusive in some cases when characteristic findings are not seen, and has to be established by surgical excision. The histopathology of the metacestode of *Cysticercus cellulosae,* as seen and illustrated by us in extraocular muscle, is very similar to the structural details reported in the CNS (25). Removal of the entire parasite results in complete cure.

References

1. Jena A, Sanchetee PC, Gupta RK, Khushu S, Chandra R, Lakshmipathi N. **Cysticercosis of the brain shown by magnetic resonance imaging**. *Clin Radiol* 1988;39:542–546
2. DiLoreto DA, Kennedy RA, Neigel JM, Rootman J. **Infestation of extraocular muscle by *Cysticercus cellulosae.*** *Br J Ophthalmol* 1990; 74:751–752
3. Escobar A, Nieto D. **Cysticercosis**. In: Minckler J, ed. *Pathology of the Nervous System*, New York, NY: McGraw-Hill; 1972;3:2507–2515
4. Sotelo J. **Neurocysticercosis**. In: Johnson R, Kennedy P, eds. *Infections of the Nervous System*. London, England: Butterworth; 1987: 145–155
5. Minguetti G, Ferreira MC. **Computed tomography in neurocysticercosis**. *J Neurol Neurosurg Psychiatry* 1983;46:936–942

6. Maschot WA. **Intraocular cysticercosis**. *Arch Ophthalmol* 1968;80: 772–774
7. Jampol LM, Caldwell JBH, Albert DM. ***Cysticercus cellulosae* in the eyelid**. *Arch Ophthalmol* 1973;89:319–320
8. Malik SRK, Gupta AK, Choudry S. **Ocular cysticercosis**. *Am J Ophthalmol* 1968;66:1168–1171
9. Perry HD, Font RL. **Cysticercosis of the eyelid.** *Arch Ophthalmol* 1978;96:1255–1257
10. Sen DK. ***Cysticercus cellulosae* in the eyelid, orbit and lacrimal gland**. *Acta Ophthalmol (Kbh)* 1980;58:144–147
11. Sing G, Kaur J. **Cysticercosis of the eyelid**. *Ann Ophthalmol* 1982; 14:947–950
12. Brooks AM, Essex WB, West RH. **Cysticercosis of superior oblique muscle**. *Aust J Ophthalmol* 1983;11:119–122
13. Rao VA, Kawatra VK, Ratnakar C. **Unusual cause of acquired inflammatory Brown's syndrome**. *Can J Ophthalmol* 1987;22:320–322
14. Malde HM, Shroff MM, Gadkari SS, Chadha D, Zankar RV. **Ocular and orbital cysticercosis**. *Australas Radiol* 1993;37:279–280
15. Suss RA, Maravilla KR, Thompson J. **MR imaging of intracranial cysticercosis: comparison with CT and anatomorphologic features**. *AJNR Am J Neuroradiol* 1986;7:235–242
16. Santain G, Vargus J. **Roentgen study of cysticercosis of the central nervous system**. *Radiology* 1966;86:520–528
17. Handler L, Mervis B. **Cerebral cysticercosis with reference to the natural history of parenchymal lesions**. *AJNR Am J Neuroradiol* 1983;4:709–712
18. Mervis B, Lotz J. **Computed tomography (CT) in parenchymal cerebral cysticercosis**. *Clin Radiol* 1980;31:521–528
19. Rodriguez-Carabajal J, Salgado P, Gutierrez R, Escobar A, Aruffo D, Palacios E. **The acute encephalitic phase of neurocysticercosis: computed tomographic manifestations**. *AJNR Am J Neuroradiol* 1983;4:51–55
20. Guilberto M, Marlus VC Ferreira. **Computed tomography in neurocysticercosis**. *J Neurol Neurosurg Psychiatry* 1983;46:936–942
21. Kramer LD, Locke GE, Byrd SE, Daryabagi J. **Cerebral cysticercosis: documentation of natural history with CT**. *Radiology* 1989; 171:459–462
22. Lotz J, Hewlett R, Alheit B, Bowen R. **Neurocysticercosis: correlative pathomorphology and MR imaging**. *Neuroradiology* 1988;30: 35–41
23. Almeida-Pinto J, Veiga-Pires JA, Stocker A, Coelho T, Monteiro L. **Cysticercosis of the brain: the value of computed tomography**. *Acta Radiol* 1988;29:625–628
24. Chang KH, Lee JH, Han MH, Han MC. **The role of contrast-enhanced MR imaging in the diagnosis of neurocysticercosis**. *AJNR Am J Neuroradiol* 1991;12:509–512
25. Vasantha S, Ravikumar BV, Roopashree SD, Das S, Shankar SK. **Neuroanatomy of *Cysticercus cellulosae* (Cestoda) as revealed by acetylcholinesterase and nonspecific esterase histochemistry**. *Parasitol Res* 1992;78:581–586